 doi:10.20944/preprints201907.0322.v1

Article

Pharmacokinetic Modeling of Ceftiofur Sodium Using Nonlinear Mixed-Effects in Healthy Beagle Dogs

Jianzhong Wang[1,2,3], Benjamin K Schneider[3], Jiao Xue[1,2], Pan Sun[1,2], Jicheng Qiu[1,2], Jonathan P. Mochel[3]* and Xingyuan Cao[1,2,4]*

[1] Department of Veterinary Pharmacology and Toxicology, College of Veterinary Medicine, China Agricultural University, People's Republic of China, Beijing 100193.
[2] Laboratory of Quality & Safety Risk Assessment for Animal Products on Chemical Hazards (Beijing), Ministry of Agriculture and Rural affairs of the People's Republic of China, Beijing 100193.
[3] Biomedical Sciences, SMART Pharmacology at Iowa State University College of Veterinary Medicine, Ames, IA, USA.
[4] Key Laboratory of Detection for Veterinary Drug Residues and Illegal Additives, Ministry of Agriculture and Rural affairs of the People's Republic of China, Beijing 100193.
* Co-corresponding/senior authors.
* Corresponding authors: Jonathan P. Mochel, Email: jmochel@iastate.edu; Xingyuan Cao, Email: cxy@cau.edu.cn

Abstract: Ceftiofur (CEF) sodium is a third-generation broad-spectrum cephalosporin commonly used in an extra-label manner in dogs for the treatment of respiratory and urinary system infections. To contribute to the literature supporting CEF use in companion animals, we have developed a compartmental, nonlinear mixed-effects (NLME) model of CEF pharmacokinetics in dogs (PK). We then used the mathematical model to predict (via Monte Carlo simulation) the duration of time for which plasma concentrations of CEF and its pharmacologically active metabolites remained above minimum inhibitory concentrations (respiratory tract *Escherichia coli spp*). Twelve healthy beagle dogs were administered either 2.2 mg/kg ceftiofur-sodium (CEF-Na) intravenously (I.V) or 2.2 mg/kg CEF-Na subcutaneously (S.C). Plasma samples were collected over a period of 72 hours post-administration. To produce a measurement of total CEF, both CEF and CEF metabolites were derivatized into desfuroylceftiofur acetamide (DCA) before analysis by UPLC-MS/MS. No adverse effects were reported after I.V or S.C dosing. The NLME PK models were parameterized using the stochastic approximation expectation maximization algorithm as implemented in Monolix 2018R2. A two-compartment mamillary model with first-order elimination and first-order S.C absorption best described the available kinetic data. Final parameter estimates indicate that CEF has a low systemic clearance (0.25 L/h/kg) associated with a low global extraction ratio E = 0.02) and a moderate volume of distribution (2.97 L/kg) in dogs. The absolute bioavailability after S.C administration was high (93.7%). Gender was determined to be a significant covariate in explaining the variability of S.C absorption. Our simulations predicted that a dose of 2.2 mg/kg CEF-Na S.C would produce median plasma concentrations of CEF of at least 0.5 μg/mL (MIC_{50}) for approximately 30 hours.

Keywords: Ceftiofur sodium; Pharmacokinetics; NLME; Beagle dogs

1. Introduction

Ceftiofur sodium (CEF-Na) is a third-generation broad-spectrum cephalosporin (β-lactam antibiotic) which is effective against Gram-positive, Gram-negative, anaerobic, and β-lactamase producing bacteria [1]. CEF has been developed and approved for treating bacterial lung diseases in cattle [2],

 doi:10.20944/preprints201907.0322.v1

swine [3] and in horses [4]. The pharmacokinetics (PK) of CEF has previously been described in cattle [5-8], camels [9], goats [10], horses [11], sheep [12], swine [1], alpacas [13], and rabbits [14].

The PK of subcutaneous (S.C) CEF crystalline-free acid S.C [15] as well as the PK of CEF-Na S.C [16] have been previously reported in dogs. However, no detailed description of CEF-Na disposition kinetics after intravenous (I.V) dosing is currently available in dogs, which prevents a rigorous assessment of absolute bioavailability in this species. And, despite common off-label use of CEF-Na in veterinary clinics for canine respiratory disease, no formulation is currently approved for use in dogs. In-depth knowledge of the time-course of systemic CEF-Na concentrations will aid in the development of effective CEF-Na formulations for the treatment of canine respiratory and urinary system infections.

The primary aim of this study was to develop a PK model of CEF disposition kinetics in healthy dogs after CEF-Na I.V and CEF-Na S.C dosing. To produce data for model building, we administered either 2.2 mg/kg CEF-Na I.V or 2.2 mg/kg CEF-Na S.C to 12 healthy beagle dogs on two separate occasions. Nonlinear mixed-effects (NLME) modeling was used for data analysis, to allow for simultaneous modeling of the I.V and S.C route. Another advantage of NLME modeling lies in the concurrent estimation of between-subject variability, within-subject (i.e. inter-occasion) variability, and individual covariate effects on drug pharmacokinetics [17-19]. After model building and validation, the resulting fit was then used to predict (via Monte Carlo simulations) the duration of time for which plasma concentrations of CEF and its pharmacologically active metabolites remained above minimum inhibitory concentrations (MIC_{50}, MIC_{90}) for Respiratory tract *Escherichia coli spp* – the most common respiratory and urinary tract pathogens in dogs.

2. Materials and Methods

2.1 Drug Supply and Animals

CEF-Na (Sterile Powder, 1 g; Lot No 1708004.2), was supplied by Qilu Animal Health Products Co., Ltd (Shandong, China). Six male and 6 female healthy beagle dogs were included in the study design. Animals ages ranged between 1.5 and 2.5 years old, while dogs weighed between 9 and 12 kg. Dogs were acclimated to the experimental facilities for a minimum of two weeks before the start of the study. They were fed with a commercial standard feed (Medium-25, Royal Canin, Shanghai, China) and had free access to fresh water. Suitability for inclusion by the study veterinarian was evaluated by physical examination combined with measurement of hematology, clinical chemistry, and coagulation time parameters. General health observations were performed at least daily. The study protocols and experimental design were reviewed and approved by the Animal Use and Care Administrative Advisory Committee of the China Agricultural University (Beijing, PR China, Ethical Protocol Code #11105-17-E-006).

2.2 Drug Administration and Sample Collection

Dogs were randomly assigned to one of two dosing groups and received either 2.2 mg/kg CEF-Na I.V or 2.2 mg/kg CEF-Na S.C – using a block design on sex to ensure that 3 males and 3 females were assigned to each study group. Approximately 2 mL of blood were collected from the cephalic vein of each dog directly into heparinized tubes at 0, 0.08 (I.V group only), 0.25, 0.5, 0.75, 1, 1.5, 2, 3, 4, 6, 8, 12, 24, 36, 48 and 72 hr post drug administration. The samples were then centrifuged at 2,280 *g* for 10 min. Plasma samples were then stored at −20°C before further analysis.**2.3 Analytical Methods**

Ceftiofur and desfuroylceftiofur metabolites in plasma samples and standards were derivatized to desfuroylceftiofur acetamide (DCA) before analysis by UPLC-MS/MS. This protocol is a modification of existing standard operating procedures for CEF quantification adapted to canine samples [6]. In this assay, dithioerythritol is used to convert ceftiofur and all desfuroylceftiofur metabolites

Preprints (www.preprints.org) | NOT PEER-REVIEWED | Posted: 28 July 2019 doi:10.20944/preprints201907.0322.v1

containing an intact β-lactam ring to desfuroylceftiofur. Desfuroylceftiofur was then stabilized by derivatization with iodoacetamide to DCA and total CEF equivalent concentration (measured as DCA) was then quantified by UPLC-MS/MS[16]. The lower limit of quantification (LLOQ) for the analysis was set at 100 ng/mL. The calibration curves were in good linearity ($R^2 > 0.998$) and ranged from 100 to 5,000 ng/mL. The inter-day and intra-day coefficients of variation – using 200, 1000, and 4000 ng/mL standards – were all below 7.58%, while the mean recoveries ranged from 82.15 to 119.44%. All analyses complied with established guidelines on bioanalytical method validation [20].

2.4 NLME Model Building and Evaluation

No outliers were identified after initial data exploration in Monolix datxplore (2018R2, Lixoft, France), such that all data could be pooled together for model building. CEF plasma concentration time-courses from I.V and S.C dosing were analyzed simultaneously using the stochastic approximation expectation maximization algorithm as implemented in Monolix 2018R2 (Lixoft, France). Individual model parameters were obtained by using the full posterior of the conditional distribution. NLME models were written as described by Sheiner and Ludden [21, 22]:

Equation 1:

$$y_{ij} = F(\phi_i, t_{ij}) + G(\phi_i, t_{ij}, \beta) \cdot \varepsilon_{ij}$$

$$\phi_i = \mu \cdot e^{\eta i}$$

$$j \in \{1, \dots, n_i\},\ i \in \{1, \dots, N\},$$

Where y_{ij} is the observed concentration of CEF equivalent collected from individual i (of N total individuals) at time t_{ij}, and j indexes the individual sample times from 1 to n_i. $F(\phi_i, t_{ij})$ is the predicted concentration of CEF at time t_{ij} dependent on ϕ_i, the vector of individual parameters (e.g. volume of distribution, clearance). $G(\phi_i, t_{ij}, \beta) \cdot \varepsilon_{ij}$ is the residual error function of $F(\phi_i, t_{ij})$ where ε_{ij} is an independent random variable distributed in a standard normal distribution i.e. $\varepsilon_{ij} \sim N(0,1)$. Each individual parameter $\theta_i \in \phi_i$ was modeled as a combination of the population mean μ (i.e. θ_{pop}) and log-normally distributed error η_i i.e. $log(\theta) \sim N(log(\mu),\ \eta_i)$.

Convergence of the SAEM algorithm was evaluated by inspection of the stability of the fixed- and random-effect parameters search as well as the precision of parameter estimates – defined via their relative standard error (RSE). Standard goodness-of-fit diagnostic plots, including individual predictions vs. observations, individual weighted residuals (IWRES), and predictions distribution were used to assess the performances of the candidate models. Normality of the random effects was assessed using the Shapiro-Wilk test as well as inspection of the full posterior distribution of random effects and residuals. Selection criteria between competing structural models included the Bayesian information criteria (BIC) and the precision of the model parameter estimates. The BIC was selected over the Akaike Information Criterion (AIC) as it tends to favor more parsimonious models [23].

Preprints (www.preprints.org) | NOT PEER-REVIEWED | Posted: 28 July 2019 doi:10.20944/preprints201907.0322.v1

2.5 Handling of Below Limit Of Quantification (BLQ) Data

Data below the LLOQ were modeled by adding to the likelihood function a term describing the probability that the true observation lies between zero and the LLOQ. For the calculation of the likelihood, this is equivalent to the M3 method implemented in NONMEM.

2.6 Random Effects Correlation Estimates

Visual inspection of the scatterplot of random effects as well as Pearson correlation tests were used to evaluate correlations between model parameters. $P < 0.05$ were considered as statistically significant. In agreement with previous literature [22, 24], several samples of the posterior distribution obtained during the last iteration of the SAEM algorithm, rather than the empirical Bayes estimate (EBE), were used when producing the scatterplot to better assess correlation between model parameters.

2.7 Inclusion of Covariate Relationships

The effect of two continuous covariates (BW and age) and one categorical covariate (sex) were evaluated using the automated Pearson's correlation test and the ANOVA method as implemented in Monolix 2018R2. $P < 0.05$ was used as threshold for statistical significance i.e. for inclusion of a covariate effect in the final NLME model. Age and BW were normalized by their median value and log-transformed during the covariate search.

2.8 Monte Carlo Simulations

The minimum plasma concentration of antimicrobial required to inhibit XX% of growth *in vitro* is known as the Minimum Inhibitory Concentration XX or MIC_{XX}. After model selection and fit, the model was used to predict for how long CEF plasma concentrations remained above the MIC_{50} (0.5 μg/mL) and MIC_{90} (8 μg/mL) for *Respiratory tract Escherichia coli spp* after administration. This time period for which concentration remained above MIC_{XX} was given the variable name τ_{XX}. MIC values were obtained from previously published canine studies [15]. The R 3.4.4 package Simulx 3.3.0 (Monolix 2018R2) was used to simulate CEF plasma disposition kinetic profiles from final Monolix run files.

In the first set of simulations, we simulated a population of 500 females and 500 females and virtually administered CEF-Na at 2.2 mg/kg S.C. Then, we used the PK data from this simulation to produce prediction distributions of CEF between 0 and 40 hours.

In the second set of simulations, we simulated the median CEF PK of male and female dogs after S.C dosing with 1 to 5 mg/kg (in steps of .1 mg/kg) of CEF-Na. Using this second simulation set, we were able to calculate the median τ_{50} and median τ_{90} for both males and females as a function of CEF-Na dosage.

3. Results

3.1 Animals

No noticeable signs of discomfort were observed upon injection of CEF-Na and no complications resulted from CEF exposure.

3.2 Pharmacokinetic Model

A total of 198 plasma concentrations of CEF and metabolites (measured as DCA by UPLC-MS/MS) from both I.V and S.C dosing groups were pooled together and simultaneously modeled using

Preprints (www.preprints.org) | NOT PEER-REVIEWED | Posted: 28 July 2019 doi:10.20944/preprints201907.0322.v1

NLME. Only 4.0 % (8/198) data were found to be below the LLOQ of the UPLC-MS/MS validated method. A two-compartment mammillary PK model with first-order elimination and first-order absorption for the S.C route, was found to best fit the pharmacokinetics of CEF equivalents in plasma based on standard goodness-of-fit diagnostic plots, precision of parameter estimates (RSE), as well as comparison of BIC between competing structural models (**Figure 1-3**) [25]. A log-normal error model best captured the residual variability in the model (**Supplemental Figure A**). Individual effects were approximately log-normally distributed around their respective population mode (**Supplemental Figure B**). After inspection of the correlation matrix of the random effects (**Figure 4**), a correlation between CEF systemic clearance (Cl) and central volume of distribution (V_1) was identified and subsequently included in the structure of the statistical model ($corr(V_1, Cl) \cong .999$, $P \leq 0.01$). Results from the automated covariate search as implemented in Monolix 2018R2 identified sex as a significant covariate on CEF subcutaneous absorption rate ($P \leq 0.01$). Gender was therefore included in the final model structure, using the following relationship:

***Equation 2**:*

$$log(ka_i) = log(ka_{pop}) + \beta \cdot sex_{i==f} + \eta_i$$

Where $sex_{i==f}$ is equal to 1 if individual i is a female and 0 otherwise. ka_{pop} is the population subcutaneous absorption rate for male dogs and β is the effect of the categorical covariate (i.e. sex) on k_a. Using final parameter estimates from the model, CEF absorption rate was estimated to be two times greater in male vs. female dogs.

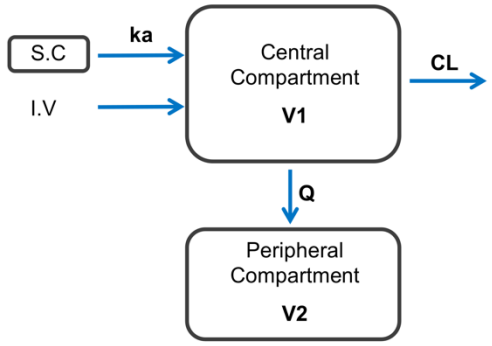

Figure 1. Schematic representation of the final model structure used to represent the dynamics of CEF following I.V and S.C dosing in healthy beagle dogs. A two-compartment pharmacokinetic model with first-order elimination and first-order absorption after S.C dosing with CEF best fitted the observed data. ka: 1-st order absorption rate following S.C dosing with CEF; CL: CEF systemic clearance; Q: inter-compartmental clearance; V1: central volume of distribution; V2: peripheral volume of distribution.

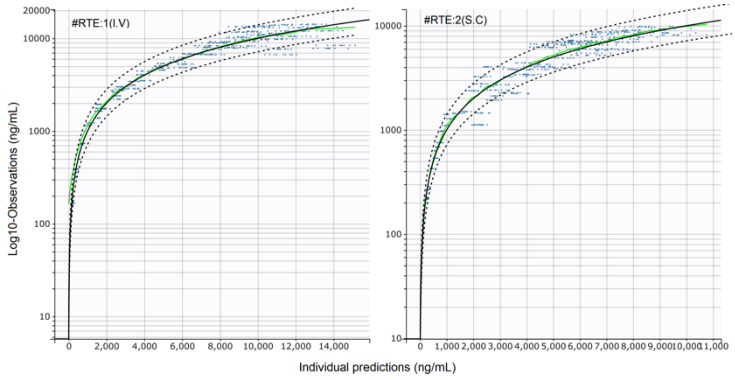

 doi:10.20944/preprints201907.0322.v1

Figure 2. Standard goodness-of-fit (sGOF) diagnostics: individual predictions vs. observations (log scale). Left panel: I.V (#RTE: 1); Right panel: S.C (#RTE: 2). The robustness of fit and predictive performances of the final model were supported by the inspection of the sGOF plots. Blue dots: observations; green line, identity line; dotted black lines: 90% prediction interval; red dots: censored (i.e. below the quantification limit) data. As described by Nguyen TH et al (25), observations were displayed on a log-scale to better evaluate the quality of fit.

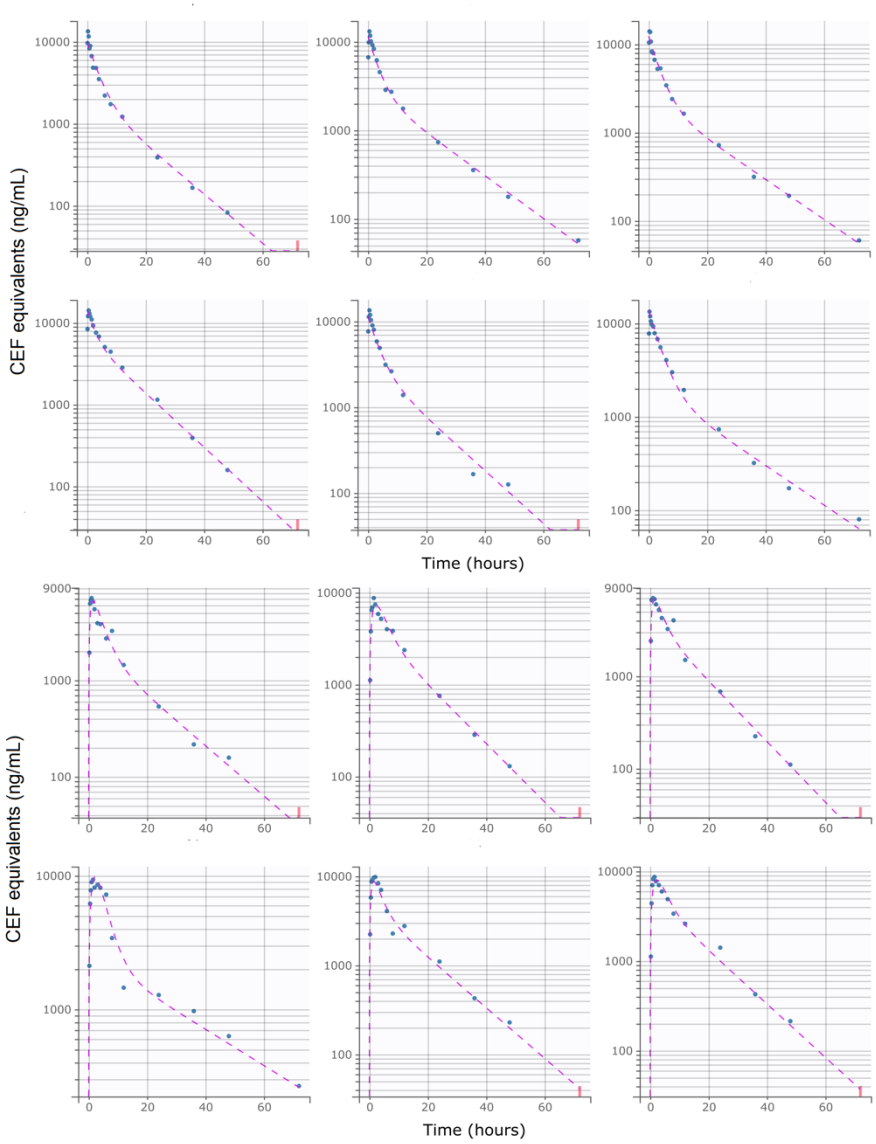

Figure 3. Individual predictions of CEF equivalent plasma concentrations in healthy beagle dogs from the final selected model. Upper panel: I.V (#RTE: 1, n=6); Lower panel: S.C (#RTE: 2, n=6). Scatter plot of observed (blue dot) and predicted (dashed purple line) individual concentration vs. time after dosing. The full model was able to describe the individual time-course of CEF equivalents for all administration schedules with excellent accuracy, as shown by the quality of the individual fits. Below LLOQ data are represented with red dots.

Preprints (www.preprints.org) | NOT PEER-REVIEWED | Posted: 28 July 2019 doi:10.20944/preprints201907.0322.v1

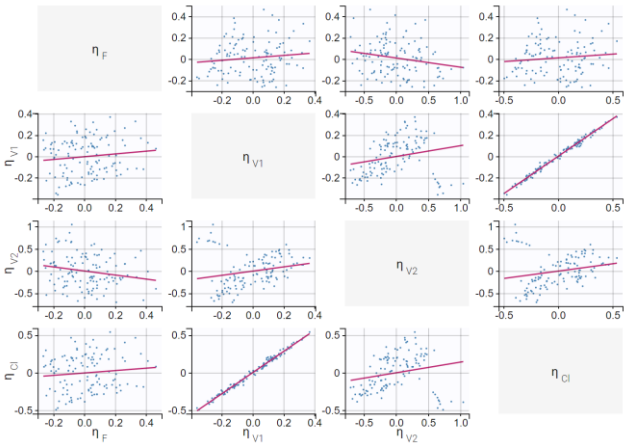

Figure 4. Correlation matrix of the random effects (i.e., the ηi). Most correlations were deemed insignificant (coefficient ≤ 0.3, P > 0.05), with the exception of the correlation between CEF clearance and volume of distribution (V1): corr_V1_Cl = 0.99 ± 0.05 (P < 0.05).

3.3 Parameters Estimates

Final parameter estimates and relevant RSEs are tabulated in **Table 1**. The precision of the final estimates was high (RSE ≤ 15%), reflecting an accurate and stable parameterization of the model. The total systemic clearance of CEF was estimated to be low 0.25 L/kg/h [26], with an estimated volume of distribution of 4.22 L/kg (2.97 and 1.25 L/kg for the volume of the central and the peripheral compartment, respectively).

Cardiac output, Q, was approximated using the formula, $Q \cong 180 \times BW^{-0.19}$ [26]. The global extraction ratio of CEF ($E = Cl/Q$) was estimated to be low ($E =$ 0.02). The absolute bioavailability of CEF was estimated as 93.7%.

Table 1. Estimated model parameters and their associated inter-individual and inter-occasion variability for CEF pharmacokinetics in dogs.

Parameter	***Symbol***	***Unit***	***Point estimate***	***Relative standard (error %)***	***IIV(%)***
Clearance	*CL*	*L/h/kg*	*0.25*	*2.0*	*24.6*
Absorption (S.C)	*Ka*	*1/h*	*1.47*	*11.9*	*--*
Central compartment volume of distribution	*V1*	*L/kg*	*1.72*	*7.3*	*18.5*
Peripheral compartment volume of distribution	*V2*	*L/kg*	*1.25*	*13.2*	*37.5*
Inter-compartmental clearance	*Q*	*L/h/kg*	*0.16*	*13.9*	*--*
Bioavailability (S.C)	*F*	*%*	*93.7*	*11.2*	*14.4*
Correlation (CL and V1)	*corr(cl_v1)*	*%*	*99.9*	*5.18*	*--*
Coefficient (Ka and sex)	β_{sex}	*-*	*-0.643*	*20.1*	*--*

IIV: Inter-Individual Variability, expressed as CV%; S.C: Subcutaneous; RSE: Relative Standard Error; --: Model parameter estimated to converge to a null value and fixed to 0. More details on the abbreviated parameters can be found in the legend of **Figure 1.**

Preprints (www.preprints.org) | NOT PEER-REVIEWED | Posted: 28 July 2019 doi:10.20944/preprints201907.0322.v1

3.4 Model Predictions

The prediction distribution of CEF equivalents over time after 2.2 mg/kg CEF-Na S.C administration suggests that CEF total concentrations (measured as DCA) would remain below the MIC_{90} concentration threshold (8 µg/mL) for most of the dosing interval, except for individuals in the upper percentiles of the simulated population (**Figure 5A**). Also, because male dogs had a higher estimated CEF absorption rate than females, their peak exposure (i.e. C_{max}) was predicted to be greater than in female dogs.

Results from our model-based simulations suggest that after one dose of 2.5 mg/kg CEF-Na S.C, ceftiofur concentrations would remain above the MIC_{50} threshold (0.5 µg/mL) for almost 1.5 days in both male and female dogs (**Figure 5B**).

In contrast, our predictions of median τ_{90} as a function of dosage indicate that even when administered at unrealistically large doses of CEF-Na S.C (~ 5 mg/kg), CEF concentrations would remain above MIC_{90} levels for no more than 8 hours (**Figure 5C**).

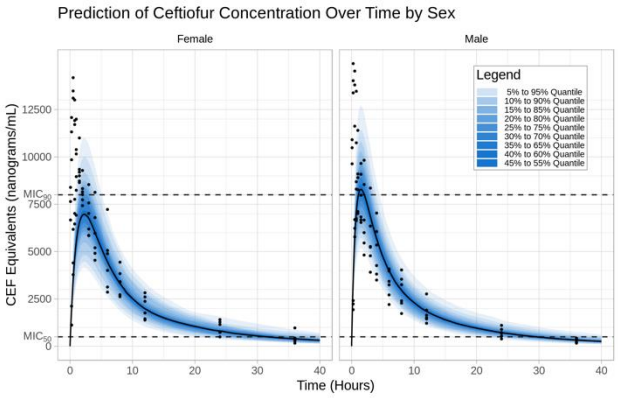

Figure 5A

Figure 5B

Figure 5C

Figure 5. A. Prediction distribution of CEF pharmacokinetics. Left panel: I.V (#RTE: 1); right panel: S.C (#RTE: 2). The theoretical distribution of CEF PK was produced by 500 Monte Carlo simulations from the final model. Briefly, the experiment was replicated virtually 500 times, allowing for each quantile (from 5 to 95 in steps of 5 i.e. {5,10,15,…,90,95}) to be estimated 500 times. The blue areas are ranges of quantiles and the blue points are observations for comparison. In a second step, simulations were used to predict for how long CEF plasma concentrations remained above the MIC50 (0.5 µg/mL) and MIC90 (8 µg/mL) for Respiratory tract Escherichia coli spp in both males and females dogs after administration CEF-Na at 2.2 mg/kg S.C. Specifically, the median PK of males and females after S.C dosing with 1 to 5 mg/kg of CEF-Na was simulated to derive the median τ50 (Figure 5B; left panel: male; right panel: female) and median τ90 (Figure 5C; left panel: male; right panel: female) as a function of CEF-Na dosage.

Preprints (www.preprints.org) | NOT PEER-REVIEWED | Posted: 28 July 2019 doi:10.20944/preprints201907.0322.v1

4. Discussion

Since 1991, Ceftiofur has been approved and extensively used by veterinarians in the treatment of bacterial infections in cattle, swine, and horses. This study constitutes the very first pharmacokinetic report of CEF-Na absolute bioavailability in dogs, allowing for the proper estimation of CEF systemic clearance and volume of distribution (as opposed to *apparent* clearance and distribution volume estimated with extravascular dosing of CEF-Na). Previously, the PK of ceftiofur in dogs has only been described in two studies. First, the PK of a single subcutaneous dose of ceftiofur crystalline-free acid has been described using noncompartmental analysis [15]. Second, the PK of CEF-Na S.C has been reported using non-linear least squares regression [16]. Results from our analysis suggest that the absolute bioavailability of CEF-Na S.C is higher in dogs than in cattle (61.12%) [6], while CEF apparent systemic clearance (CL/F) is lower in dairy cows vs. dogs (0.12 vs. 0.26 L/h/kg) [6].

In our analysis, CEF and desfuroylceftiofur metabolites (containing an intact β-lactam ring) in plasma samples were derivatized to DCA [16], and total CEF equivalent concentrations (measured as DCA) were quantified by UPLC-MS/MS. Free concentrations only accounts for about 10% of total CEF equivalents[6]. However, protein binding of desfuroylceftiofur is known to be reversible, such as protein-bound desfuroylceftiofur acts as a reservoir for release of active therapeutic drug at the site of infection [27]. Hence, measurement of DCA regardless of protein binding was used for simulation of *what-if* scenarios and dose optimization in our experiment.

NLME models are a versatile statistical tool for quantifying variability in drug disposition as a function of individual patient characteristics (i.e. covariates, such as age, sex and bodyweight) [28-30]. NLME modeling also enables decoupling of intra-individual variability, inter-individual variability, and residual error. This allows to individually consider the many factors that could affect drug exposure in any given individual. Pooling data from I.V and S.C dosing with CEF (totaling 198 concentrations), the disposition kinetics of CEF equivalents was best modeled using a two-compartmental mammillary model with first-order elimination and first-order absorption from the S.C injection site. Our final selected model precisely captured the individual PK of total CEF equivalents over time in both dosing groups. Results from the automated covariate analysis in Monolix 2018R2 further suggest that sex has a significant effect (β_{sex} = -0.643 ± 20.1%) on CEF absorption rate following subcutaneous administration. This was also supported by the inspection of the distribution of the estimated individual absorption parameters (i.e. ka_i). Specifically, CEF absorption rate was estimated to be two times greater in male vs. female dogs, and our model-based simulations confirmed the potential need for dose adjustment based on sex in dogs. To the best of our knowledge, no previous studies had reported an effect of sex on ceftiofur PK in dogs or any other species.

Importantly, using final parameters estimates from the NLME model, we could simulate '*what-if*' scenarios to evaluate various dosing schedules for CEF-Na S.C in dogs. The most important risk factor for emergence of resistance is repeated exposure of bacteria to suboptimal concentrations of antimicrobials related to the selection of inappropriate dosing schedules [30]. As a cephalosporin antibiotic, CEF exhibits time-dependent bactericidal activity i.e. plasma concentrations of CEF must be maintained over relevant MIC levels for an extended period of time. As such, the amount of time that CEF concentrations remain above the MIC_{XX} (i.e. τ_{xx}) is the PK-PD best index for predicting drug efficacy [31].

According to previous research with cephalosporins, τ_{xx} should be at least 50% (and preferably ≥ 80%) of the dosage interval to achieve optimal bactericidal effect without inducing resistance [32].

Based on these guidelines, our simulations predict a spectrum of viable dosing regimens for CEF-Na subcutaneous in dogs for *Escherichia coli spp*. However, producing a definitive recommendation of dosing interval for CEF in dogs was not within the primary scope of this study. As such, further

 doi:10.20944/preprints201907.0322.v1

studies in client-owned animals with clinical disease are required to validate and build on our preliminary findings in healthy dogs.

5. Limitations

Our study had several limitations. First, this experiment was performed in healthy dogs and model-based predictions of CEF disposition kinetics may not extend to dogs with bacterial infection, impaired hepatic function, or impaired renal function. Second, we chose to refer to MIC values from previous studies rather than culturing clinical pathogens as a part of the sampling process. Finally, and with respect to our experimental design, this study solely reports the disposition kinetics of CEF after a single dose of CEF-Na, with no information about systemic accumulation and steady-state pharmacokinetics of CEF in dogs.

Supplementary Materials: The following are available online at 10.5281/zenodo.3348395, Figure A and Figure B.

Author Contributions: All authors contributed to the preparation of the manuscript. XC and JW were involved in the original design and execution of the study. PS, JX, JW and JQ were responsible for the animal experiments. BS, JW and JPM performed the NLME data analysis and wrote the manuscript. All authors have read and approved the final version of the manuscript.

Funding: This work was supported by the National Science & Technology Pillar Program during the Thirteenth Five-Year Plan Period (2016YFD0501309-1) and the National Natural Science Foundation of China (No. 31672599).

Acknowledgments: We would like to thank Shuyuan Li for her technical assistance with the analytical determination of CEF.

Conflicts of Interest: The authors declare no conflicts of interest.

 doi:10.20944/preprints201907.0322.v1

References

1. Brown, S.A., et al., Comparison of plasma pharmacokinetics and bioavailability of ceftiofur sodium and ceftiofur hydrochloride in pigs after a single intramuscular injection. Journal of Veterinary Pharmacology and Therapeutics, 1999. 22(1): p. 35-40.
2. FDA, Implantation injectable dosage form; animal drugs not subject to certification ceftiofur sterile powder. 1991. p. 12119 %\ 2015-12-09 07:50:00.
3. FDA, Original new animal drug application ¥Ceftiofur h ydrochloride Sterile suspension for injection swine and cattle (beef, non-lactating dairy, and lactating dairy) NADA 141-288 %\ 2016-01-31 20:40:00. 2008.
4. Hall, T.L., et al., Pharmacokinetics of ceftiofur sodium and ceftiofur crystalline free acid in neonatal foals. J Vet Pharmacol Ther, 2011. 34(4): p. 403-9.
5. Soback, S., S. Bright, and M. Paape, Disposition kinetics of ceftiofur in lactating cows. Acta Veterinaria Scandinavica, 1991(Supplementum 87): p. 93-95.
6. Wang, J., et al., Pharmacokinetic profile of Ceftiofur Hydrochloride Injection in lactating Holstein dairy cows. Journal of Veterinary Pharmacology and Therapeutics, 2018. 41(2): p. 301-306.
7. Brown, S.A., S.T. Chester, and E.J. Robb, Effects of age on the pharmacokinetics of single dose ceftiofur sodium administered intramuscularly or intravenously to cattle. Journal of Veterinary Pharmacology and Therapeutics, 1996. 19(1): p. 32-38.
8. Gorden, P.J., et al., Comparative plasma and interstitial fluid pharmacokinetics and tissue residues of ceftiofur crystalline-free acid in cattle with induced coliform mastitis. J Vet Pharmacol Ther, 2018. 41(6): p. 848-860.
9. Goudah, A., Pharmacokinetics of ceftiofur after single intravenous and intramuscular administration in camels (Camelus dromedarius). J Vet Pharmacol Ther, 2007. 30(4): p. 371-4.
10. Courtin, F., et al., Pharmacokinetics of ceftiofur and metabolites after single intravenous and intramuscular administration and multiple intramuscular administrations of ceftiofur sodium to dairy goats. Journal of Veterinary Pharmacology and Therapeutics, 1997. 20(5): p. 368-73.
11. Collard, W.T., et al., Pharmacokinetics of ceftiofur crystalline-free acid sterile suspension in the equine. Journal of Veterinary Pharmacology and Therapeutics, 2011. 34(5): p. 476-481.
12. Craigmill, A.L., et al., Pharmacokinetics of ceftiofur and metabolites after single intravenous and intramuscular administration and multiple intramuscular administrations of ceftiofur sodium to sheep. Journal of Veterinary Pharmacology and Therapeutics, 1997. 20(2): p. 139-144.
13. Dechant, J.E., et al., Pharmacokinetics of ceftiofur crystalline free acid after single and multiple subcutaneous administrations in healthy alpacas (Vicugna pacos). J Vet Pharmacol Ther, 2013. 36(2): p. 122-9.
14. Gardhouse, S., et al., Pharmacokinetics and safety of ceftiofur crystalline free acid in New Zealand White rabbits (Oryctolagus cuniculus). Am J Vet Res, 2017. 78(7): p. 796-803.
15. Hooper, S.E., et al., Pharmacokinetics of Ceftiofur Crystalline-Free Acid in Clinically Healthy Dogs (Canis lupus familiaris). J Am Assoc Lab Anim Sci, 2016. 55(2): p. 224-9.
16. Brown, S.A., et al., Plasma and urine disposition and dose proportionality of ceftiofur and metabolites in dogs after subcutaneous administration of ceftiofur sodium. Journal of Veterinary Pharmacology and Therapeutics, 1995. 18(5): p. 363-369.
17. Pillai, G.C., F. Mentre, and J.L. Steimer, Non-linear mixed effects modeling - from methodology and software development to driving implementation in drug development science. J Pharmacokinet Pharmacodyn, 2005. 32(2): p. 161-83.
18. Mochel, J.P. and M. Danhof, Chronobiology and Pharmacologic Modulation of the Renin-Angiotensin-Aldosterone System in Dogs: What Have We Learned? Rev Physiol Biochem Pharmacol, 2015. 169: p. 43-69.
19. Bon, C., et al., Mathematical modeling and simulation in animal health. Part III: Using nonlinear mixed-effects to characterize and quantify variability in drug pharmacokinetics. J Vet Pharmacol Ther, 2018. 41(2): p. 171-183.
20. FDA, Guidance for Industry: Bioanalytical Method Validation [Draft Guidance](2013). 2013, Department of Health and Human Services, Food and Drug Administration, Center for Drug Evaluation and Research (CDER), Center of Veterinary Medicine (CVM).
21. Sheiner, L.B. and T.M. Ludden, Population pharmacokinetics/dynamics. Annu Rev Pharmacol Toxicol, 1992. 32: p. 185-209.

22. Pelligand, L., et al., Modeling of Large Pharmacokinetic Data Using Nonlinear Mixed-Effects: A Paradigm Shift in Veterinary Pharmacology. A Case Study With Robenacoxib in Cats. CPT Pharmacometrics Syst Pharmacol, 2016. 5(11): p. 625-35.
23. Mould, D.R. and R.N. Upton, Basic concepts in population modeling, simulation, and model-based drug development-part 2: introduction to pharmacokinetic modeling methods. CPT Pharmacometrics Syst Pharmacol, 2013. 2(4): p. e38.
24. Lavielle, M. and B. Ribba, Enhanced Method for Diagnosing Pharmacometric Models: Random Sampling from Conditional Distributions. Pharm Res, 2016. 33(12): p. 2979-2988.
25. Nguyen, T.H., et al., Model Evaluation of Continuous Data Pharmacometric Models: Metrics and Graphics. CPT Pharmacometrics Syst Pharmacol, 2017. 6(2): p. 87-109.
26. Toutain, P.L. and A. Bousquet-Melou, Plasma clearance. J Vet Pharmacol Ther, 2004. 27(6): p. 415-25.
27. Clarke, C.R., et al., Penetration of parenterally administered ceftiofur into sterile vs. Pasteurella haemolytica-infected tissue chambers in cattle. J Vet Pharmacol Ther, 1996. 19(5): p. 376-81.
28. Fink, M., et al., Population pharmacokinetic analysis of blood concentrations of robenacoxib in dogs with osteoarthritis. Res Vet Sci, 2013. 95(2): p. 580-7.
29. Riviere, J.E., et al., Mathematical modeling and simulation in animal health. Part I: Moving beyond pharmacokinetics. J Vet Pharmacol Ther, 2016. 39(3): p. 213-23.
30. Toutain, P.-L. and A. Bousquet-Melou, How antibiotic dosage regimens based on PK-PD concepts may be an important contribution to the resistance problem. 2019.
31. Nielsen, E.I., O. Cars, and L.E. Friberg, Pharmacokinetic/pharmacodynamic (PK/PD) indices of antibiotics predicted by a semimechanistic PKPD model: a step toward model-based dose optimization. Antimicrob Agents Chemother, 2011. 55(10): p. 4619-30.
32. Toutain, P.L., J.R.E. del Castillo, and A. Bousquet-Mélou, The pharmacokinetic–pharmacodynamic approach to a rational dosage regimen for antibiotics. Research in Veterinary Science, 2002. 73(2): p. 105-114.